PHOTOINDUCED ORDERING OF LAMELLAR *n*-ALKYLSILOXANE FILMS

Lingli Ni[1*], Abraham Chemtob[1], Céline Croutxé-Barghorn[1], Jocelyne Brendlé[2], Loïc Vidal[2], Séverinne Rigolet[2]

[1]*Laboratory of Photochemistry and Macromolecular Engineering, ENSCMu,University of Haute-Alsace, 3 rue Alfred Werner 68093 Mulhouse Cedex, France*
[2]*Institut de Science des Matériaux de Mulhouse, Mulhouse, LRC-CNRS, 7228,ENSCMu, University of Haute-Alsace, 3 rue Alfred Werner 68093 Mulhouse Cedex, France*
E-mail: lingli.ni@uha.fr

Keywords: Self-organization, Photopolymerization, sol-gel

Abstract
Self-assembled organosilica films exhibiting various lamellar structures were prepared without solvent and water via the fast photoacid-catalyzed sol-gel process of n-octadecyltrichlorosilanes (C_{18}TCS) and n-alkyltrimethoxysilanes (C_nTMS, n = 8, 10, 12, 16 and 18). This facile photochemical route towards nanostructured hybrid films relies on superacid photocatalyst generated by the UV photolysis of a soluble lipophilic iodonium salt: $(C_{12}H_{25})_2\Phi_2I^+$ SbF_6^-. The effect of the alkyl chain length and the type of silyl functionality on the level of ordering of the layered mesostructure (short- or long-range order), the alkyl chain packing arrangement and its conformational order have been studied via various characterization techniques (XRD, SEM, TEM, solid state NMR, etc.).

1 Introduction

Organic-inorganic hybrids with ordered nanostructure represent an attractive class of materials endowed with a wide range of potential applications in polymer nanocomposites[1], catalysis[2], optoelectronics[3] and photolithography[4]. Surprisingly, most of these crystalline hybrids were accessed via a sol-gel process despite its well-known propensity to afford amorphous silica and metal oxide structures. Up to now, few long-range organized hybrids have been reported in the literature, mainly, through the selection of suitable organosilane precursors and specific experimental parameters: temperature, solvent, catalyst, etc.[5] Two synthetic pathways were used essentially: surfactant templating to afford hybrid mesoporous or microporous solids[6] and supramolecular self-assembly arising from weak interactions between condensed organosilane molecules[7]. The first one requires template extraction after synthesis to exploit the nanostructuration as well as complex experimental conditions to emerge the hybrid character (post-functionalization or organosilane co-condensation). Another limitation is a periodicity originating from the pores and scarcely from the hybrid framework itself (walls), which remains in most instances amorphous.
In the second approach, the organic moiety of the organosilane induces a self-organization during polycondensation without directing agent to yield long-range organized polysilsesquioxanes with a periodicity assigned this time to the regular arrangement of the

organic units. The key feature is a self-organization driven by the development of weak interactions (i.e., Van der Waals, π- π stacking and H-bonding) between specific organic substituents during the precursor's hydrolysis and polycondensation.[8] The main effort has been focused on bis-silylated trialkoxysilanes [$(R'O)_3Si\text{-}R\text{-}Si(OR')_3$],[7] leading to various nano and microscale structures, such as helical fibers[9], hollow tubes[10], spheres[10] and lamellae[11]. In contrast, self-organization of dissymmetric mono-silylated organic precursors [$RSi(OR')_3$] is more challenging, as evidenced by the weak number of studies devoted to this subject.[8c, 12] However, the majority of the hybrid products usually derive in this case from gel and are thus obtained in a bulk or particle form, which is a limitation for their practical applications.[3c, 13] The only exceptions were the nanostructured films developed by Kuroda et al. using a mixture of tetramethoxysilane (TMOS) and *n*-alkyltrialkoxysilane precursors.[14] Their studies demonstrated the formation of well-ordered multilayered films due to the combined networking ability of TMOS and the self-assembly property of the long *n*-alkylsilane.[14b] Yet, the polymerization of this bi-component system is slow, kinetically driven and a precise control of the processing and chemical conditions turned out to be necessary to achieve a long-range organization.[15] In addition, the films remained poorly condensed in most cases and the limited solubility of the *n*-alkylsilanes was a severe hurdle that obstructed further investigation.

In this study, we present the formation of lamellar hybrid thin films derived from a series of *n*-alkyltrichlorosilanes (C_{18}TCS) and *n*-alkyltrimethoxysilane precursors (C_nH_{2n+1}TMS, n = 8-18 denoted C_nTMS). Our procedure uses a fast water and solvent-free sol-gel photopolymerization catalyzed by the *in situ* photogeneration of $H^+SbF_6^-$ Brönsted superacids resulting from the UV decomposition of a lipophilic diphenyliodonium salt: $(C_{12}H_{25})_2\Phi_2\text{-}I^+$ SbF_6^-. A main emphasis has been on discussing the effect of the alkyl chain length and the type of silyl functionality on the level of ordering of the layered mesostructure (short- or long-range order), the alkyl chain packing arrangement (bilayered or interdigitated) and its conformational order (*gauche*, *trans*). To this end, extensive characterization of the resulting poly(*n*-alkylsilsesquioxane) (C_nPS) films was performed using X-ray diffraction and electron microscopy,. Further, the combination of different solid-state NMR techniques (^{29}Si, ^{13}C) shed light into the siloxy layer microstructure and the conformational structure of the alkyl chain respectively.

2 Experimental section

In a typical procedure, photoacid generator UV1241 (2 % wt.) and benzophenone (2 % wt.) were dissolved in the C_{18}TCS or C_nTMS precursor (n = 8, 10, 12, 16 or 18) to form a photolatent solution in the absence of UV light. Then the resulting formulation was deposited on a glass substrate previously treated by 20 % wt. NaOH solution using an Elcometer 4340 automatic film applicator equipped with a wire wound bar to produce a 5 µm thick liquid film. Irradiation was performed at room temperature under a UV conveyor with a belt speed of 10 m/min using a microwave lamp (H lamp, Fusion), light intensity: 1.46 J/cm^2 per pass). The samples were subjected to 5 successive passes under the conveyor to yield transparent solid poly(*n*-alkylsilsesquioxane) film labelled as $C_{18}PS_{TCS}$ or C_nPS_{TMS}, whatever the alkyl chain length. During UV irradiation, the room humidity was maintained between 30-35 % with a hygrometer. The resulting samples were then characterized by a range of techniques: solid state NMR, X-ray diffraction and electron/polarized optical microscopy.

3 Results and discussion

3.1 Photoinduced ordering of C_{18}TCS

As displayed in Scheme 1, the generally accepted mechanism of onium salt-type photoinitiator photolysis first involves the generation of a series of photoproducts (cations,

radicals, radical cationic species) resulting from the homolytic and heterolytic Φ-I bond cleavage. The resulting cationic species interact with hydrogen donors, such as precursor molecules or impurities, to create Brönsted acid of the structure H^+X^- ($H^+SbF_6^-$ in our case) based on a weakly coordinating anion X^-. These protonic superacids are thought to play a prominent role in the catalysis of the sol-gel process. As onium salts weakly absorb at $\lambda > 300$ nm in a region where the UV lamp emits predominantly, a benzophenone acting as a photosensitizer was added in conjunction with the iodonium salt. Upon irradiation, benzophenone mainly absorbs the light at 313 and 360 nm emitted by the Hg-Xe lamp and efficiently transfers the energy to the diaryl iodonium salt.

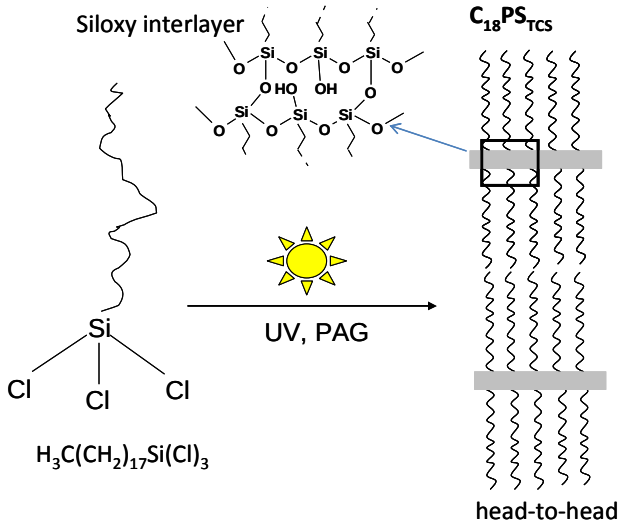

Scheme 1. Representation of the photoinduced sol-gel synthesis and ordering of C_{18}TCS process

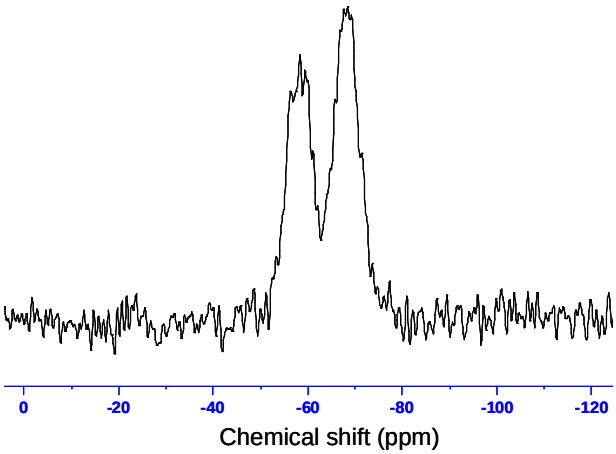

Figure 1. ^{29}Si Solid state SPE-MAS NMR spectrum of UV-cured $C_{18}PS_{TCS}$ films.

Quantitative solid-state ^{29}Si single pulse magic angle spinning (SPE-MAS) NMR experiments were conducted to examine the siloxy microstructure in more detail. As shown in Figure 1, the ^{29}Si MAS spectrum of $C_{18}PS_{TCS}$ displays only T^2 ($(HO)(R)Si(OSi)_2$, -57.9 ppm) and T^3 ($(R)Si(OSi)_3$, 68.1 ppm) siloxane species. The proportion of each siloxane subspecies determined by peak ratios deconvolution and integration led to a proportion of 45 and 55 % respectively, which suggests that the photoinduced sol-gel reaction proceeded efficiently. The high cross-linking was also exemplified by the excellent film chemical resistance in various conventional solvents (THF, CH_2Cl_2, etc) and a gel content of 100 %.

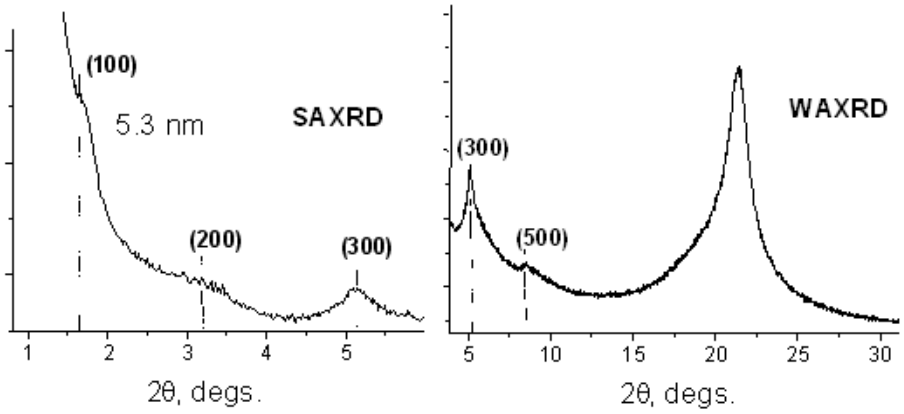

Figure 2. XRD spectra of $C_{18}PS_{TCS}$ films (a: small angle; b: wide angle)

As shown in Figure 2, the small-angle (SAXS) and wide-angle X-ray powder diffraction (WAXRD) patterns of scratched $C_{18}PS_{TCS}$ film give four orders of (l00) peaks which can be readily assigned to the bilayer structure with d spacing of 53.4 Å. This interlamellar distance slightly deviates from the theoretical value of 52.4 Å predicted by molecular modelling for the double layer structure with highly trans $C_{18}H_{37}$ chains oriented normal to the siloxane layer. Figure 3 displayed a TEM image of the hybrid UV-cured film confirms the sheet-like structure. Well defined parallel stripes are observed with an interlamellar distance estimated between 46-53 Å. A systematic analogy can be drawn with organo-clays structures, which are actually the archetype of layered organic-inorganic hybrids.

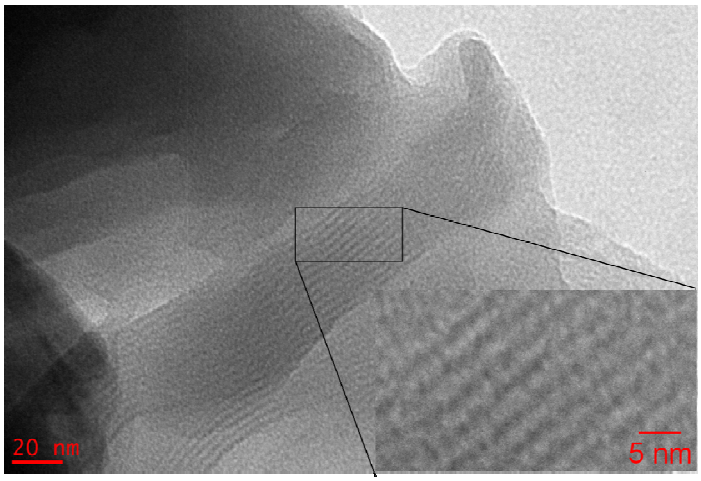

Figure 3. TEM image of $C_{18}PS_{TCS}$ films synthesized via sol-gel photopolymerization

Since the early work from Earl and Ando, it has been well established that microstructural changes in the average local alkane chain conformation are manifested as different ^{13}C chemical shifts of the methylene carbons. In methylene-rich polymers such as polyethylene, this phenomenon is called the γ-gauche shielding effect. The crystalline carbons (33-34 ppm) in the all-trans, planar zigzag conformation resonate 3-4 pmm downfield from the amorphous portions possessing some *gauche* character (30 ppm). As can be seen in Figure 4, the ^{13}C cross polarization (CP) MAS NMR spectrum of $C_{18}PS_{TCS}$ shows two components assigned to the 14 interior CH_2 carbons (C_3-C_{16}) in the 28-37 ppm range: the most intense signal located at 33.3 ppm arises from *trans* conformers while the second one at 30.8 ppm indicates the existence of *gauche* defects. By comparison, the C_{18}TCS liquid precursor displays a complete

conformational disorder with only the peak at 30 ppm remaining, which indicates equilibrium between *trans* and *gauche* conformers.

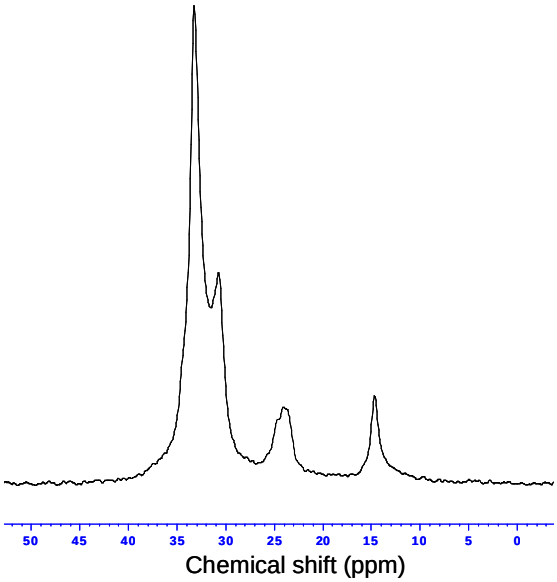

Figure 4. ^{13}C Solid state CP-MAS NMR spectra of $C_{18}PS_{TCS}$

3.2 Alkyl chain length effect with C_nTMS precursors

Figure 5 displays the SAXS (a) and WAXRD (b) patterns of the hybrid films derived from C_nTMS. The shape and position of low angle scattering peaks (d_{00l}) are informative of the level of ordering and the packing arrangement of the interlayer alkyl chains (Fig 5a). For $n \leq 12$, d-spacings values of 1.99, 2.13 and 2.40 nm were obtained respectively for samples C_8PS, $C_{10}PS$ and $C_{12}PS$. It is worth noting the relative correspondence with the theoretical values of 2.32, 2.92 and 3.25 nm predicted for the bilayer structure ($2l$) with n = 8, 10 and 12: $CH_3(CH_2)_nSiO_x\text{-}O_xSi(CH_2)_nCH_3$, from molecular modelling where l is the length of a fully extended trans carbon chain including the contribution of the siloxy part. We assume that the structure of the poly(*n*-alkylsiloxane) films consists of bilayered stacks of alkyl chains with an interlayer composed of partially cross-linked $SiO_x(OH)_{3-x}$ sheets. In all cases however, the absence of sharp Bragg signal and reflections orders ruled out the occurrence of crystal organization, the presence of a broad signal being more indicative of a short-range order. The observed layer thickness ($l < d < 2l$) differ somehow from the estimated values because of this local ordering as well as the conformational disorder of these short alkyl chains with probably a significant fraction of gauche defects[13]. A bilayered structuration presumably occurs although a small interpenetration of the hydrocarbon and a tilted angle of the layer structure cannot be ruled out.

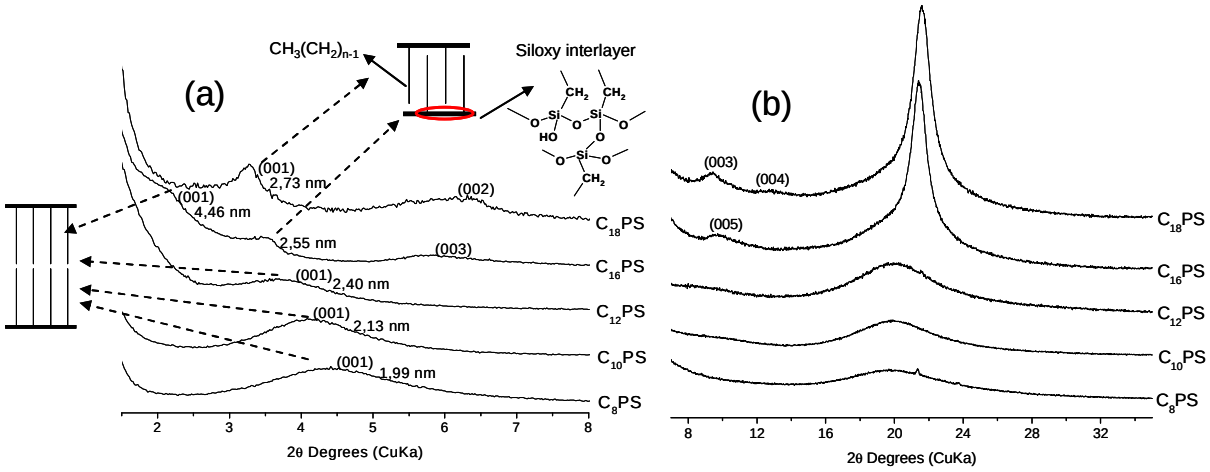

Figure. 5 XRD spectra of C_nPS_{TMS} films (a: small angle; b: wide angle)

Significant changes in the SAXS and XRD patterns were observed upon increasing the alkyl chain length to n = 16 and 18. In contrast to the previous samples, $C_{16}PS$ was characterized by two distinct d-spacings at 2.55 and 4.46 nm. The extended chain length of $C_{16}H_{33}SiO_x$ unit (*l* = 2,37 nm) suggests in this case the presence of two different lamellar organizations: The higher value is consistent with a bilayer structure as reported for shorter hydrocarbon units, while the smaller distance is indicative of a coexisting interdigitated monolayer structure. In the surfactant literature, head to head bilayered and head to tail interdigitated structures are known as the two archetypes of amphiphilic lamellar phases. The dependence of the interlayer structure with chain length was confirmed with the examination of the $C_{18}PS$ films. When the carbon chain length was increased to 18, we only observed a single d-spacing value at 2.73 nm in agreement with the extended chain length of $C_{18}H_{37}SiO_x$ unit at 2.62 nm, which indicates in this case a complete interdigitated monolayer phase with alternating up and down alkyl chains. The close proximity between the experimental and the theoretical values for n = 16 and 18 presumably translates a higher conformational order of the alkyl chain. In addition, these polysilsesquioxane films were characterized by thinner Bragg peaks and several reflection peaks at intermediate scattering angles, indicating a long-range periodicity. In both cases, the peaks observed at higher angles are attributable to higher order diffractions, suggesting a high level of ordering. $C_{18}PS$ showed for example a well-developed progression of reflections at 27.3, 13.8, 9.2 and 6.8 nm associated to the first, second, third and forth order (Fig 5a and 5b).

3.3 Influence of the hydrolysable function

Figure 6 displays the SAXS patterns of the $C_{18}PS_{TCS}$ and $C_{18}PS_{TMS}$ hybrid films, derived respectively from C_{18}TCS and C_{18}TMS sol-gel photopolymerization. Both patterns are consistent with a multilayer mesostructure composed of alkyl chains bilayers separated by siloxy sheets. Despite their relative broadness, the presence of several peaks at the intermediate scattering angles suggests a long-range periodicity.[33] The major difference between the films prepared from alkoxy and chloro precursors appears in the position of the low angle diffraction peak (d_{001}), translating a distinct packing arrangement of the hybrocarbon chains forming the interior bilayer. Compared to the theoretical length of a fully extended $C_{18}H_{37}SiO_x$ unit (*l* = 2.62 nm), the *d*-spacing value of 5.3 nm (~2×*l*) found with $C_{18}PS_{TCS}$ can be related to a conventional bilayer organization with a head-to-head arrangement. In the case of $C_{18}PS_{TMS}$, the distance of 2.73 nm, close to the theoretical chain length, suggests distinctively fully interdigated bilayers with alternating up-and-down octadecyl chains.

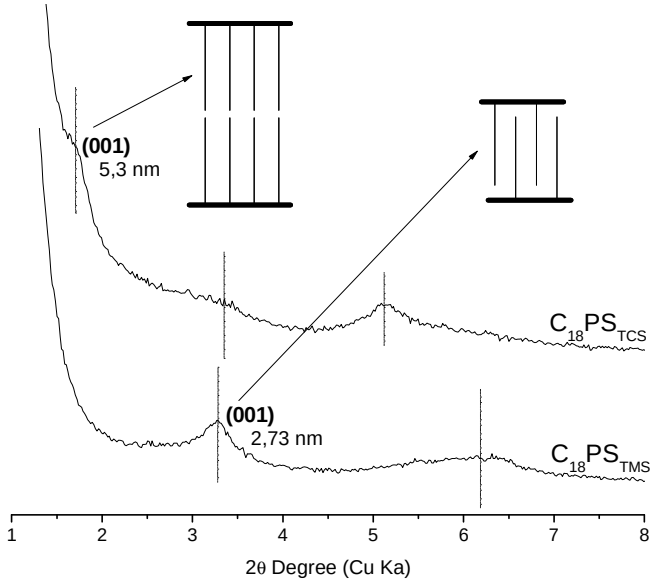

Figure 6. SAXS spectra of $C_{18}PS_{TCS}$ and $C_{18}PS_{TMS}$ films

4 Conclusion

A novel route towards crystalline layered poyl(*n*-alkylsilsesquioxane) films was described that sheds light on new aspects of this long-range ordered hybrid, first synthesized in the late nineties. The developed sol-gel methodology merely relies on Brönsted superacids photocatalysts released by the UV illumination of a lipophilic diphenyl iodonium salt. Of particular interest is that the described photopolymerization and self-assembly process proceeds in bulk without any solvent and water, thus obviating the insolubility problem of the *n*-alkysilanes precursors. Although a classical hydrolytic mechanism takes place here, the reaction was carried out by simple diffusion of moisture diffusion within the precursor film to ensure hydrolysis, thereby avoiding its premature precipitation. Extensive characterization (XRD, TEM, solid-state NMR) highlighted that both supramolecular and conformational orders were dependent upon the alkyl chain length and the nature of hydrolysis functional groups. The longer alkylene units exhibit more cohesive Van der Waals interactions between chains, which has a strong impact on the extent of ordering. Only long-range ordered mesostructures were achieved with C_{18}TCS, C_{16} and C_{18}TMS precursors, although a distinct packing arrangement was reported in each case: a single interdigitated lamellar structure or head to head bilayer structure when n = 18 (hydrolysis functional dependent) versus a bilayered-interdigitated mixture with n = 16..

Reference

[1] W.L. Ijdo, T. Lee and T.J. Pinnavaia, *Adv. Mater.*, 1996, **8**, 79.
[2] J. Alauzun, A. Mehdi, C. Reye and R.J.P. Corriu, *Chem. Commun.*, 2006, 347.
[3] (a) A.B. Bourlinos, S.R. Chowdhury, D. Jiang, Y. An, Q. Zhang, L.A. Archer and E.P. Giannelis, *Small*, 2005, **1**, 80; (b) H. Peng, Y. Zhu, D. Peterson and Y. Lu, *Adv. Mater.*, 2008, **20**, 1199; (c) M. Takahashi, C. Figus, T. Kichob, S. Enzo, M. Casula, M. Valentini and P. Innocenzi, *Adv. Mater.*, 2009, **21**, 1732.
[4] (a) C.S. Dulcey, J.H. Georger, M. Chen, S.W. McElvany, C.E. O'Ferrall, V.E. Benezra and J.M. Calvert, *Langmuir*, 1996, **12**, 1638; (b) X. Sallenave, O.J. Dautel, G. Wantz, P. Valvin, J.P. Lère-Porte and J.J.E. Moreau, *Adv. Funct. Mater.*, 2009, **19**, 404.
[5] B. Menaa, M. Takahashi, P. Innocenzi and T. Yoko, *Chem. Mater.*, 2007, **19**, 1946.

[6] (a) C.E. Fowler, S. L. Burkett and S. Mann, *Chem. Commun.*, 1997, 1769; (b) C. Sanchez, C. Boissiere, D. Grosso, C. Laberty and L. Nicole, *Chem. Mater.*, 2008, **20**, 682.
[7] S. Fujita and S. Inagaki, *Chem. Mater.*, 2008, **20**, 891.
[8] (a) F. Lerouge, G. Cerveau and R.J.P. Corriu, *New. J. Chem.*, 2006, **30**, 1364; (b) B. Boury and R.J.P. Corriu, *Chem. Rec.*, 2003, **3**, 120; (c) A. Mehdi, *J. Mater. Chem.*, 2010, **20**, 9281.
[9] J.J.E. Moreau, L. Vellutini, M. Wong Chi Man, C. Bied, J.L. Bantignies, P. Dieudonne and J.L. Sauvajol, *J. Am. Chem. Soc.*, 2001, **123**, 7957.
[10] J.J.E. Moreau, L. Vellutini, M. Wong Chi Man and C. Bied, *Chem. Eur. J.*, 2003, **9**, 1594.
[11] J.J.E. Moreau, B. Pichon, M. Wong Chi Man, C. Bied, H. Pritzkow, J.L. Bantignies, P. Dieudonné and J.L. Sauvajol, *Angew. Chem., Int. Ed.*, 2004, **116**, 205.
[12] (a) A.N. Parikh, M.A. Schivley, E. Koo, K. Seshadri, D. Aurentz, K. Mueller and D.L. Allara, *J. Am. Chem. Soc.*, 1997, **119**, 3135; (b) A. Shimojima and K. Kuroda, *Chem. Rec*., 2006, **6**, 53; (c) R. Mouawia, A. Mehdi, C. Reye and R.J.P. Corriu, *J. Mater. Chem.*, 2007, **17**, 616; (d) A. Shimojima, C.W. Wu and K. Kuroda, *J. Mater. Chem.*, 2007, **17**, 658; (e) J. Jiang, O.V. Lima, Y. Pei, X. Zeng, L. Tian and E. Forsythe, *J. Am. Chem. Soc.*, 2009, **131**, 900; (f) Q. Ke, J. Li, Y. Liu, T. He and X. Li, *Langmuir*, 2009, **26**, 3579.
[13] A. Shimojima and K. Kuroda, *Langmuir*, 2002, **18**, 1144.
[14] (a) A. Shimojima, Y. Sugahara and K. Kuroda, *J. Am. Chem. Soc.*, 1998, **120**, 4528; (b) A. Shimojima, N. Umeda and K. Kuroda, *Chem. Mater.*, 2001, **13**, 3610.
[15] Y. Fujimoto, A. Shimojima and K. Kuroda, *Chem. Mater.*, 2003, **15**, 4768.